EUROPEAN LABORATORY FOR PARTICLE PHYSICS (CERN)

ALEPH 99-049
CONF 99-025
TAMPERE ABSTRACT# 6-429
30th June 1999

PRELIMINARY

Single- and multi-photon production in e^+e^- collisions at a centre-of-mass energy of 188.6 GeV

The ALEPH Collaboration

Abstract

The production of final states involving only one or more energetic photons from e^+e^- collisions is studied in a sample of $173.6\,pb^{-1}$ of data recorded at a centre-of-mass energy of 188.6 GeV by the ALEPH detector at LEP. The $e^+e^- \to \nu\bar{\nu}\gamma(\gamma)$ and $e^+e^- \to \gamma\gamma(\gamma)$ cross sections are measured. The data are in good agreement with predictions based on the Standard Model and are used to set upper limits on the cross sections for additional photon production in the context of supersymmetric models, anomalous WWγ couplings and for various extensions to QED. In particular, in the context of a super-light gravitino model a cross section upper limit of 0.27 pb is placed on the process $e^+e^- \to \tilde{G}\tilde{G}\gamma$, allowing a 95% C.L. lower limit of $1.0 \times 10^{-5}\,eV/c^2$ to be set on the mass of the gravitino. In the framework of anomalous WWγ couplings, the parameters $\Delta\kappa_\gamma$ and λ_γ are measured to be $0.4 \pm 0.7(stat) \pm 0.2(syst)$ and $0.3 \pm 0.9(stat) \pm 0.2(syst)$, respectively. In the case of equal $ee^*\gamma$ and $ee\gamma$ couplings a 95% C.L. lower limit on M_{e^*} of $335\,GeV/c^2$ is obtained.

(ALEPH contribution to the 1999 summer conferences)

Contact: Gary.Taylor@cern.ch

1 Introduction

In the framework of the Standard Model, events in which the only observable final state particles are photons may be produced via two distinct reactions: $e^+e^- \to \nu\bar{\nu}\gamma(\gamma)$ and $e^+e^- \to \gamma\gamma(\gamma)$.

The reaction $e^+e^- \to \nu\bar{\nu}\gamma(\gamma)$ can proceed via two processes which are theoretically well understood: radiative returns to the Z resonance ($e^+e^- \to \gamma Z$) with $Z \to \nu\bar{\nu}$, and t-channel W exchange with photon(s) radiated either from the beam electrons or from the virtual W (giving access to the tri-linear WWγ couplings). This reaction produces final states where one or more photons are accompanied by significant missing energy. These final states have been studied extensively in e^+e^- annihilations at lower centre-of-mass energies [1, 2]. Such final states are also sensitive to new physics via the reactions $e^+e^- \to XX$ and $e^+e^- \to XY$ where Y is purely weakly interacting and X decays radiatively to Y ($X \to Y\gamma$). In the Minimal Supersymmetric Standard Model (MSSM) Y and X could be the lightest and next-to-lightest neutralinos [3, 4, 5], respectively. In Gauge Mediated Supersymmetry Breaking (GMSB) theories [6] Y and X could be the essentially massless gravitino and the lightest neutralino [7, 8], respectively. Searches for such GMSB topologies are presented in [9]. In the super-light-gravitino scenario [10] the process $e^+e^- \to \tilde{G}\tilde{G}\gamma$ can have an appreciable cross section.

The CDF collaboration has observed an unusual event with two high energy electrons, two high energy photons, and a large amount of missing transverse energy [11]. The Standard Model explanation for this event has a low probability, but it can be accommodated by the MSSM as outlined below. The D0 collaboration has also searched for this process [12] and has found no significant excess of events. In the neutralino LSP scenario, the CDF event could be explained by the Drell-Yan process $q\bar{q} \to \tilde{e}\tilde{e} \to ee\chi_2^0\chi_2^0 \to ee\chi_1^0\chi_1^0\gamma\gamma$ [5] where the two χ_1^0's escape detection, resulting in missing transverse energy. If this is the explanation for the CDF event, the best possibility for discovery at LEP2 is $e^+e^- \to \chi_2^0\chi_2^0 \to \chi_1^0\chi_1^0\gamma\gamma$. Limits derived from the ALEPH data are compared to the regions favoured by the CDF event within this model. In gravitino LSP models, the CDF event could be explained by $q\bar{q} \to \tilde{e}\tilde{e} \to ee\chi_1^0\chi_1^0 \to ee\tilde{G}\tilde{G}\gamma\gamma$ [8]. In this scenario the best channel for discovery at LEP2 is $e^+e^- \to \chi_1^0\chi_1^0 \to \tilde{G}\tilde{G}\gamma\gamma$. Searches for this process are presented in [9].

In e^+e^- collisions at LEP 2 energies, the trilinear WWγ and WWZ couplings can be probed with direct W-pair ($e^+e^- \to W^+W^-$) production, single W ($e^+e^- \to We\nu$) production or with photon production ($e^+e^- \to \nu\overline{\nu}\gamma(\gamma)$). In the WW channel a minimal set of five independent parameters is necessary to describe the Z and γ couplings to the W, assuming C and CP conservation. Usually a model-dependence is introduced to reduce this set to at most three parameters (e.g. the model with the parameters $\alpha_W, \alpha_{W\phi}, \alpha_{B\phi}$ [13]). Although the photonic channel is less sensitive to the couplings than the W pair and single W channels, it can resolve sign ambiguities and is therefore complementary. Constraints on the WWγ vertex have previously been obtained both at LEP2 [14] and at the Tevatron [15] (within a slightly different theoretical framework). The description of the Standard Model processes involved in the reaction ($e^+e^- \to \nu\overline{\nu}\gamma(\gamma)$ and the definition of the measured trilinear gauge couplings can be found in [16].

The reaction $e^+e^- \to \gamma\gamma(\gamma)$ proceeds via t-channel electron exchange and has been studied at lower centre-of-mass energies [1, 17]. Deviations from the expected QED differential cross section for the production of two photons could be evidence for new physics due to, for example, $e^+e^-\gamma\gamma$ contact interactions or excited electrons.

This paper is based on an analysis of $173.6\,\mathrm{pb}^{-1}$ of data recorded at a centre of mass energy of 188.6 GeV Previously published results from ALEPH [1, 16] based on $11.1\,\mathrm{pb}^{-1}$, $10.6\,\mathrm{pb}^{-1}$and $58.5\,\mathrm{pb}^{-1}$ of data taken at 161 GeV, 172 GeV and 182.7 GeV, respectively, are taken into account

when setting cross section limits on new physics processes.

2 The ALEPH detector and photon identification

The ALEPH detector and its performance are described in detail elsewhere [18, 19]. The analysis presented here depends largely on the performance of the electromagnetic calorimeter (ECAL). The tracking system, composed of a silicon vertex detector, wire drift chamber, and time projection chamber (TPC), is used to provide efficient ($> 99.9\%$) tracking of isolated charged particles in the angular range $|\cos\theta| < 0.96$. The luminosity calorimeters (LCAL and SICAL), together with the hadron calorimeter (HCAL), are used mainly to veto events in which photons are accompanied by other energetic particles. The SICAL provides coverage between 34 and 63 mrad from the beam axis while the LCAL provides coverage between 45 and 160 mrad. Each LCAL endcap consists of two halves which fit together around the beam axis; the area where the two halves join is a region of reduced sensitivity ("the LCAL crack"). This vertical crack, which accounts for only 0.05% of the total solid angle coverage of the ALEPH detector, was instrumented with a veto counter for the 183 GeV run. This counter consists of 2 radiation lengths of lead followed by scintillation counters. Energetic electrons (photons) passing through the lead have a greater than 90% (70%) chance of giving a veto signal in the scintillation counters. The HCAL is instrumented with streamer tubes and, together with the muon chambers, is used to identify muons.

The ECAL is a lead/wire-plane sampling calorimeter consisting of 36 modules, twelve in the barrel and twelve in each endcap, which provide coverage in the angular range $|\cos\theta| < 0.98$. Inter-module cracks reduce this solid angle coverage by 2% in the barrel and 6% in the endcaps. However, the ECAL and HCAL cracks are not aligned so there is complete coverage in ALEPH down to 34 mrad. At normal incidence the ECAL comprises a total thickness of 22 radiation lengths and is situated at 185 cm from the interaction point. Anode wire signals, sampled every 512 ns during their rise time, provide a measurement by the ECAL of the interaction time t_0 of the particles relative to the beam crossing with a resolution better than 15 ns for showers with energy greater than 1 GeV. Cathode pads associated with each layer of the wire chambers are connected to form projective "towers", each subtending approximately $0.9^\circ \times 0.9^\circ$. Each tower is read out in three segments in depth, "storeys", of four, nine and nine radiation lengths. The high granularity of the calorimeter provides excellent identification of photons and electrons. The energy deposited in the calorimeter is measured on both the cathode pads and anode wires. This redundancy is useful in providing an accurate energy measurement in the small number of cases where storeys are not functioning due to electronics problems. The energy calibration of the ECAL is obtained from Bhabha events, two-photon events and events from two-photon interactions. The energy resolution is measured to be $\Delta E/E = 0.18/\sqrt{E} + 0.009$ (E in GeV) [19].

Photon candidates are identified using an algorithm [19] which performs a topological search for localised energy depositions within groups of neighbouring ECAL towers. In order to optimise the energy reconstruction, photons that are not well-contained in the ECAL (near or in a crack) have their energy measured from the sum of the localised energy depositions and all energy deposits in the HCAL within a cone of $\cos\alpha > 0.98$. Photon candidates may also be identified in the tracking system if they convert in the material before the TPC, 6% of a radiation length at normal incidence, producing an electron-positron pair [19].

The trigger most relevant for photonic events is the neutral energy trigger. This trigger is based on the total energy measured on the wires of each of the ECAL modules. For the 188.6 GeV run, this trigger accepts events if the total wire energy is at least 1 GeV in any barrel module or

at least 2.3 GeV in any endcap module. The efficiency of this trigger for the selections presented below is estimated to be at least 99.8%.

3 The Monte Carlo samples

The efficiency for the $e^+e^- \to \nu\bar{\nu}\gamma(\gamma)$ cross section measurement and the background for the anomalous photon plus missing energy searches are estimated using the KORALZ Monte Carlo program [20]. This generator uses the YFS [21] approach to explicitly generate an arbitrary number of initial state photons. It has been modified to treat the effects of photons produced as a result of bremsstrahlung off the exchanged virtual W. This treatment includes the expected standard model contribution as well as possible anomalous couplings together with their possible interference. Although the effect on the overall cross section measured below is expected to be small (0.2%), the corrections in certain kinematical regions can be as large as a few percent. The KORALZ Monte Carlo is checked by comparing to an independent generator NUNUGPV [22] which is based on exact lowest order amplitudes for the production of up to three photons in the final state, modified for higher order QED effects using transverse momentum dependent structure functions. The effect of missing higher order electroweak correction, which are not treated by either generator, is estimated to be less than 1%.

The efficiency estimates for the reaction $e^+e^- \to \gamma\gamma(\gamma)$ are obtained using the GGG generator [23] which contains contributions to order α^3 with both soft and hard photon emission. Events with four hard photons observed in the detector are simulated using an order α^4 generator [24]. The efficiencies for the processes $e^+e^- \to XX$ and $e^+e^- \to XY$ with $X \to Y\gamma$ are estimated using SUSYGEN [25] assuming isotropic production and decay of X and taking into account the effects of initial state radiation.

Background from Bhabha scattering, where initial or final state particles radiate a photon is studied using the BHWIDE [26] Monte Carlo program.

4 One photon and missing energy

4.1 Event selection

The selection of events with one photon and missing energy follows that of the previous ALEPH analyses [1] and only a brief summary is given here. Events are selected with no charged tracks (unless they come from an identified conversion) and exactly one photon inside the acceptance cuts of $|\cos\theta| < 0.95$ with $p_\perp > 0.0375\sqrt{s}$ (where $p_\perp$ is defined as the measured transverse momentum relative to the beam axis). Cosmic ray events that traverse the detector are eliminated by the charged track requirement or if there are hits in the outer part of the hadron calorimeter HCAL. Residual cosmic ray events and events with detector noise in the electromagnetic calorimeter ECAL are removed by selection criteria based on the ECAL information. The "impact parameter of the photon", calculated using the barycentre of the photon shower in each of the three ECAL storeys, is required to be less than 25 cm. The compactness of the shower in the ECAL is calculated by taking an energy-weighted average of the angle subtended at the interaction point between the cluster barycentre and the barycentre of each of the ECAL storeys contributing to the cluster. The compactness is required to be less than 0.85°. The interaction time of the event is required to be within 60 ns of a beam crossing.

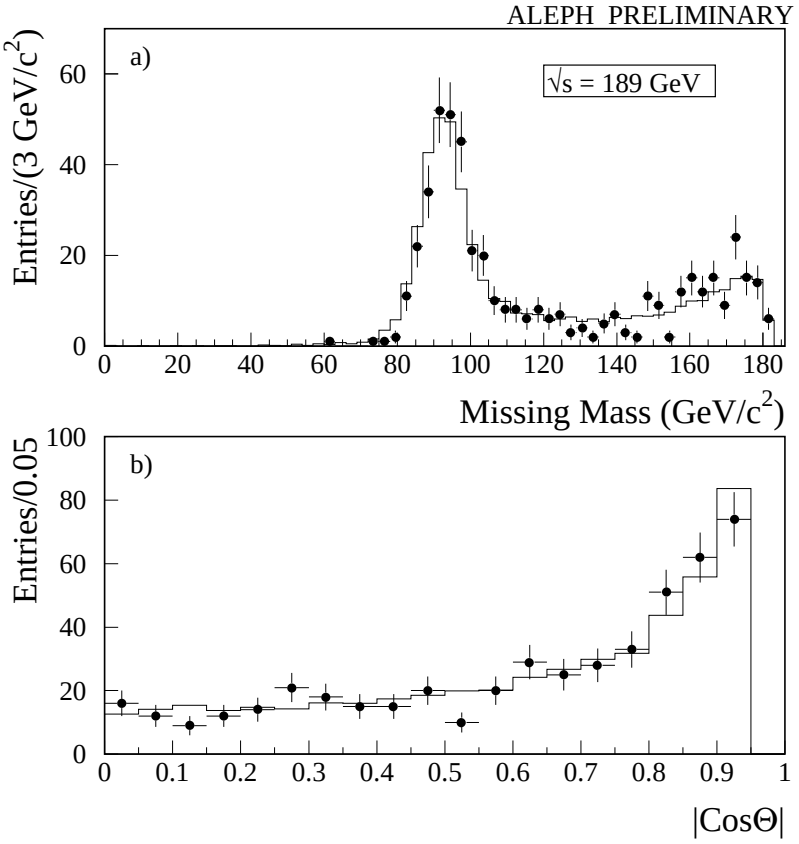

Figure 1: *a) The invariant mass distribution of the system recoiling against the photon candidate is shown for the data (points with error bars) and Monte Carlo (histogram). b) The polar angle distribution is shown for the data (points with error bars) and Monte Carlo (histogram).*

To suppress background from Bhabha scattering, events are required to have no energy deposited within 14° of the beam axis and to have less than 1 GeV of non-photonic energy.

4.2 Measurement of the $e^+e^- \to \nu\bar{\nu}\gamma(\gamma)$ cross section

The efficiency of the above selection for the process $e^+e^- \to \nu\bar{\nu}\gamma(\gamma)$ is estimated from the Monte Carlo to be 74%. This efficiency includes a 5% loss, due to uncorrelated noise or beam-related background in the detector, estimated using events triggered at random beam crossings.

When this selection is applied to the data, 484 one-photon events are found. The KORALZ Monte Carlo predicts that 492 events would be expected from Standard Model processes. The cross section to have at least one photon inside the acceptance $|\cos\theta| < 0.95$ and $p_\perp > 0.0375\sqrt{s}$ is measured to be

$$\sigma(e^+e^- \to \nu\bar{\nu}\gamma(\gamma)) = 3.78 \pm 0.17 \pm 0.11\,\text{pb}.$$

The missing mass and polar angle distributions of the selected data events are in good agreement with the Monte Carlo expectations as shown in Figure 1.

The estimate of the systematic uncertainty in the above cross section measurement includes contributions from the sources listed in Table 1. The simulation of the energetic photon shower is

Table 1: *Systematic uncertainties for the one-photon channel.*

Source	Uncertainty (%)
Photon selection	0.6
Converted photon selection	0.3
Background	<0.6
Integrated luminosity	0.5
Monte Carlo theoretical	1.4
Monte Carlo statistical	0.4
Total (in quadrature)	1.8

checked with a sample of Bhabha events selected requiring two collinear beam-momentum tracks and using muon chamber information to veto $\mu^+\mu^-$ events. The tracking information is masked for these events and the above photon reconstruction is redone. The efficiency to reconstruct a photon in the data is found to be consistent at the 0.6% level with the simulated prediction. The uncertainty in the number of simulated pair conversions is estimated to give a 0.3% change in the overall efficiency. The 0.7% energy calibration uncertainty is found to have a negligible effect. The level of cosmic ray and detector noise background is measured by looking for events slightly out-of-time with respect to the beam crossing. No out-of-time events are observed in a time window five times larger than that used in the selection. This leads to an estimate of less than 0.6 events expected at 95% C.L. in the selected sample. The residual background from Bhabha scattering is estimated from Monte Carlo studies and is found to be negligible. From a comparison of different event generators [20, 22] the theoretical uncertainty on the selection efficiency, including the effect of missing higher order electroweak diagrams, is estimated to be less than 1.4%. The total systematic uncertainty is obtained by adding in quadrature the individual contributions.

4.3 Search for the process $e^+e^- \to XY \to YY\gamma$

In order to search for the signal $e^+e^- \to XY \to YY\gamma$, a two-dimensional binned maximum likelihood fit is performed on the observed missing mass versus polar angle two dimensional distribution under the hypothesis that there is a mixture of signal and background in the data. Details of the fitting procedure are given in Ref. [1]. Data recorded at lower centre-of-mass energies are included in the fit with a β/s cross section dependence. The fit is performed for all possible X,Y mass combinations in steps of $1\,\mathrm{GeV}/c^2$ and the resulting upper limits on the cross section at 95% C.L. are shown in Figure 2.

4.4 Search for the process $e^+e^- \to \tilde{G}\tilde{G}\gamma$

If the gravitino $\tilde{G}$ is very light the cross section for the process $e^+e^- \to \tilde{G}\tilde{G}\gamma$ can become appreciable. In order to search for this process a binned maximum likelihood fit is performed as above. In this case the missing mass and polar angle distributions of the signal together with the cross section dependence on the centre-of-mass energy are calculated from the differential cross section given in Ref. [10]. The systematic uncertainty of 1.8% is taken into account in the fit. From the fit a cross section limit of 0.27 pb at $\sqrt{s} = 188.6\,\mathrm{GeV}$ is obtained at 95% C.L. This results in a 95% C.L. lower limit of $1.0 \times 10^{-5}\,\mathrm{eV}/c^2$ for the mass of the gravitino [10]. In the same paper a more general approach gives a mass limit dependent on two free parameters. In the worst case

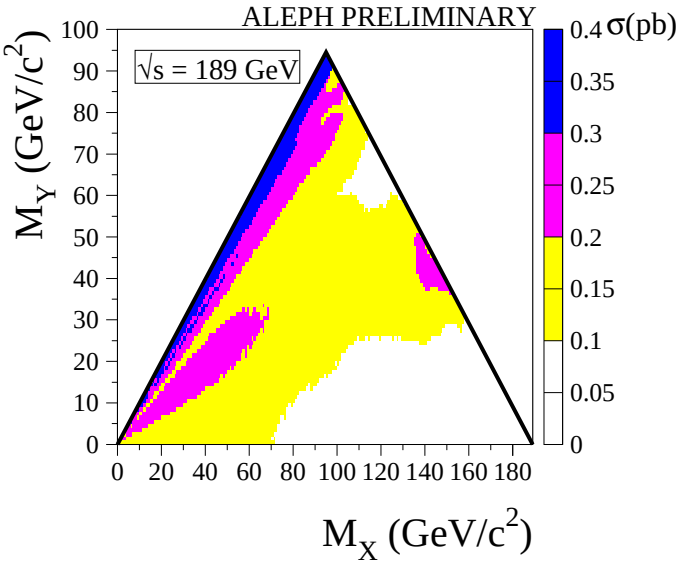

Figure 2: *The 95% C.L. upper limit on the production cross section in pb for the process* $e^+e^- \to XY \to YY\gamma$. *The limits are valid for* $\sqrt{s} = 188.6\,\text{GeV}$ *assuming a* β/s *threshold dependence, isotropic production and decay, short X lifetime* ($\tau_X < 0.1\,\text{ns}$) *and* 100% *branching ratio for* $X \to Y\gamma$.

this would lead to a limit on the gravitino mass lower by a factor of two.

5 Two photons and missing energy

5.1 Event preselection

Events with two photons and missing energy are expected to be produced via the reaction $e^+e^- \to \nu\bar{\nu}\gamma\gamma(\gamma)$. Events are selected with no charged tracks (not coming from a conversion) and at least two photons, with energy above 1 GeV, inside the acceptance of $|\cos\theta| < 0.95$. Since at least two photons are required, background from cosmic rays and detector noise is less severe, so the impact parameter and compactness requirements are not imposed. Events with more than two photons are required to have at least $0.4\sqrt{s}$ of missing energy. Background from the process $e^+e^- \to \gamma\gamma(\gamma)$ is effectively eliminated by requiring that the acoplanarity of the two most energetic photons be less than 177° and that there be less than 1 GeV of additional visible energy in the event. The total $p_\perp$ is required to be greater than 3.75% of the missing energy, reducing background from radiative events with final state particles escaping down the beam axis to a negligible level.

When this selection is applied to the 188.6 GeV data, 21 events are selected while 27 are predicted from the process $e^+e^- \to \nu\bar{\nu}\gamma\gamma(\gamma)$. From a comparison of different event generators [20, 22] the theoretical uncertainty on this prediction, including the effect of missing higher order

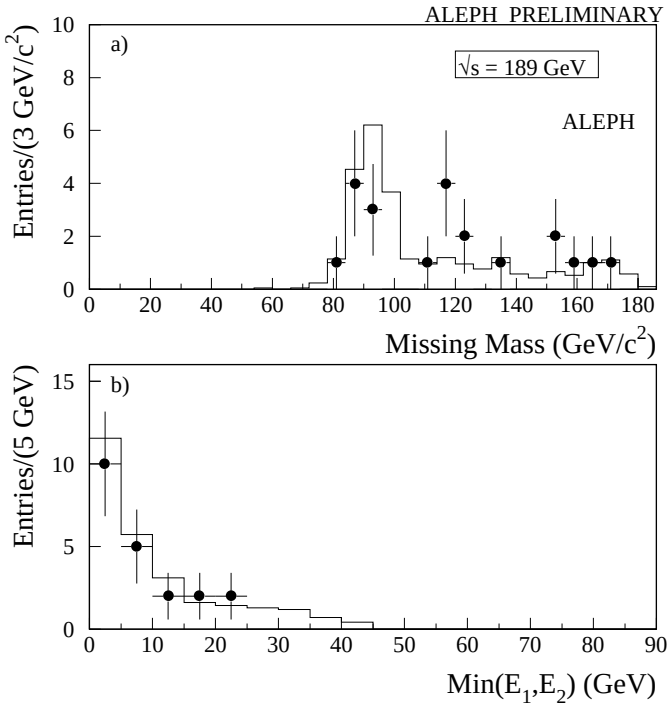

Figure 3: *a) The invariant mass distribution of the system recoiling against the photon candidates is shown for the data (points with error bars) and Monte Carlo (histogram). b) The distribution of the energy of the second most energetic photon is shown for the data (points with error bars) and Monte Carlo (histogram).*

electroweak diagrams, is estimated to be less than 1.4%. The missing mass and the energy of the second most energetic photon of these selected data events are shown together with Monte Carlo expectations in Figure 3.

5.2 Search for the process $e^+e^- \to XX \to YY\gamma\gamma$

To search for the $e^+e^- \to XX \to YY\gamma\gamma$ process the fact that the $e^+e^- \to \nu\bar{\nu}\gamma\gamma(\gamma)$ background peaks at small polar angles and has a missing mass near the Z mass is utilised. Events with a missing mass close to the Z mass (between $82\,\mathrm{GeV}/c^2$ and $100\,\mathrm{GeV}/c^2$) and the energy of the second most energetic photon less than 10 GeV are rejected. The $\cos\theta$ cut is set using the $\bar{N}_{95}$ procedure [27], leading to a requirement of $|\cos\theta| < 0.8$. When this selection is applied to the 188.6 GeV data 5 events are selected while 7.4 events are expected from the $e^+e^- \to \nu\bar{\nu}\gamma\gamma(\gamma)$ process. The upper limits obtained on the cross section as a function of the masses of X and Y are shown in Figure 4. These upper limits are derived without performing background subtraction but the observed candidates are taken into account only where they are kinematically consistent with a given X,Y mass pairing. The limits take into account lower energy data [1] with a β/s threshold dependence and assuming a branching ratio for $X \to Y\gamma$ of 100%. The systematic uncertainty on the efficiency of this analysis is estimated to be less than 2% and the effect on the upper limits is less than 1%.

The χ_1^0 LSP interpretation of the CDF event (along with the non-observation of other SUSY signatures at Fermilab) suggests a high branching ratio for $\chi_2^0 \to \chi_1^0\gamma$. A 100% branching ratio is

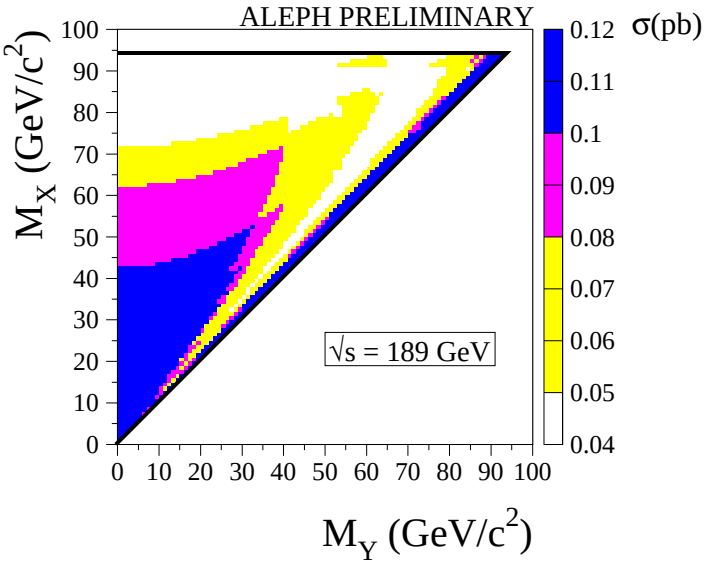

Figure 4: *The 95% C.L. upper limit on the production cross section in pb for the process* $e^+e^- \to XX \to YY\gamma\gamma$ *multiplied by* $\mathcal{B}(X \to Y\gamma)$ *squared. The limit is valid for* $\sqrt{s} = 188.6\,\text{GeV}$ *assuming* β/s *threshold behaviour and isotropic decays.*

achieved when the χ_2^0 is pure photino and the χ_1^0 is pure higgsino. In this scenario, the lower mass limit of χ_2^0 as a function of the selectron mass is calculated and compared to the region compatible with the CDF event. In Figure 5 two scenarios $M_{\tilde{e}_L} = M_{\tilde{e}_R}$ and $M_{\tilde{e}_L} \gg M_{\tilde{e}_R}$ are shown. With the assumption that the χ_2^0 is pure photino and the χ_1^0 is pure higgsino, these results exclude a large fraction of the region compatible with the kinematics of the CDF event given by the neutralino LSP interpretation.

6 WWγ couplings from $e^+e^- \to \nu\overline{\nu}\gamma(\gamma)$

Events with one or more photons and missing energy may also be used to probe the anomalous WWγ coupling parameters $\Delta\kappa_\gamma$ and λ_γ. Events sensitive to these couplings are selected by requiring, in addition to the requirements of sections 3.1 and 4.1, that there be at least one photon in the event with $\theta_\gamma > 20^\circ$ and $p_{T\gamma}/E_{beam} > 0.1$. Furthermore events where a photon has converted into a e^+e^- pair are not considered. For this analysis the photon energy is based on the energy measurement from the ECAL clusters, as described in [16]. With the above selection criteria 378 events are selected in the data while 381 would have been expected from Standard Model processes. Of these, two have two photons while 4.9 would have been expected from standard processes.

Information on anomalous couplings are extracted from the data by performing a generalised maximum likelihood fit based on the overall number of observed photons and on their polar angles θ_γ and scaled energies x_E. Defining $E_\gamma^Z = (s - m_Z^2)/2\sqrt{s}$, the fit is performed separately in the

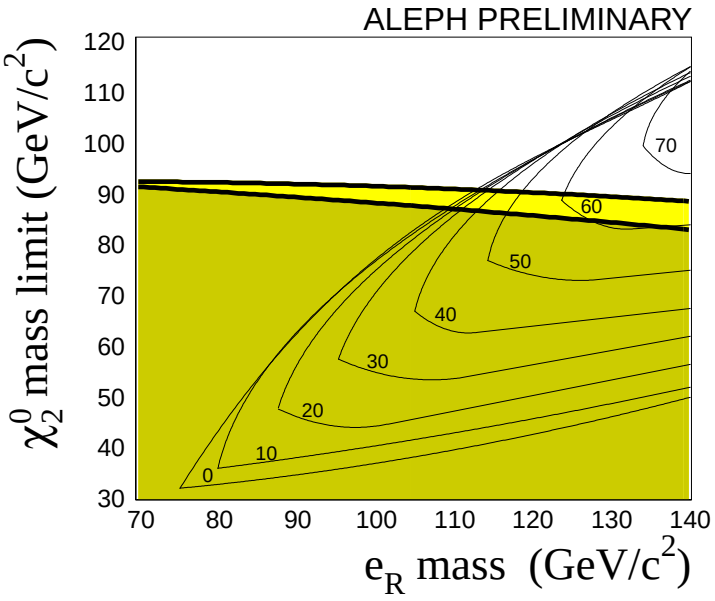

Figure 5: *The excluded region in the neutralino, selectron mass plane at 95% C.L. For this plot it is assumed that the χ_2^0 is pure photino and that the χ_1^0 is pure higgsino which implies $\mathcal{B}(\chi_2^0 \to \chi_1^0\gamma) = 1$. The lightly shaded region is for $M_{\tilde{e}_L} = M_{\tilde{e}_R}$. The darker shaded region refers to $M_{\tilde{e}_L} \gg M_{\tilde{e}_R}$. The mass limit is independent of the χ_1^0 mass as long as the $\chi_2^0 - \chi_1^0$ mass differences is greater than 25 GeV/c^2. Overlayed is the CDF region labelled by the mass of χ_1^0 in GeV/c^2. This is the area determined from the properties of the CDF event assuming the reaction $q\bar{q} \to \tilde{e}\tilde{e} \to ee\chi_2^0\chi_2^0 \to ee\chi_1^0\chi_1^0\gamma\gamma$ (taken from Ref. [5]).*

following two kinematic regions:

- Region 1, low energy photons with $E_\gamma < E_\gamma^Z - 3\Gamma_Z$

  The contribution from higher order radiative corrections is described by an almost constant term obtained from the Monte Carlo simulation. The scaled variable x_E is found to be as discriminant as the angular variable in the fit. Both are used for the $\Delta\kappa_\gamma$ fit, whereas λ_γ is determined only from the total cross section. The sensitivity to the λ_γ parameter in this kinematic region is very low [16].

- Region 2, high energy photons with $E_\gamma > E_\gamma^Z - 3\Gamma_Z$

  In this region, the higher order radiative corrections decrease the number of expected photons by 30%. The scaled energy x_E is more discriminant than the angular variable, both variables being used in the fit of $\Delta\kappa_\gamma$ and λ_γ. It can be observed that the sensitivity to λ_γ with x_E is similar to that of $\Delta\kappa_\gamma$.

The generalised likelihood is of the form

$$\log\mathcal{L} = \log\frac{(N_{th}^{(1)})^{N_{obs}^{(1)}}\, e^{-N_{th}^{(1)}}}{N_{obs}^{(1)}!} + \log\frac{(N_{th}^{(2)})^{N_{obs}^{(2)}}\, e^{-N_{th}^{(2)}}}{N_{obs}^{(2)}!} + \sum \log P_i^{(1)} + \sum \log P_i^{(2)},$$

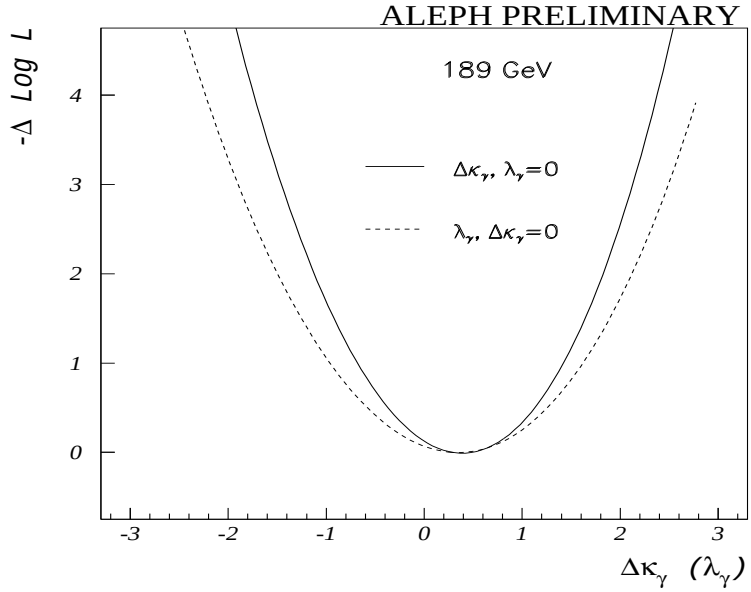

Figure 6: Likelihood curves for the fit of λ_γ at $\Delta\kappa_\gamma = 0$ (solid curve) and $\Delta\kappa_\gamma$ at $\lambda_\gamma = 0$ (dashed curve) for the sum of the cross section and distribution shape terms.

where $\mathrm{P}_\mathrm{i}^{(1)}$, $\mathrm{P}_\mathrm{i}^{(2)}$ are the probability density functions of observing photon i with a given value of x_E and θ_γ in region 1 and 2 respectively, and $\mathrm{N}_\mathrm{th}^{(1)}$ and $\mathrm{N}_\mathrm{th}^{(2)}$ are the expected number of photons in each region, including background. The number of photons used in the fit is 120 (expected 128) and 260 (expected 258) in regions 1 and 2, respectively.

6.1 Results of the fit

The likelihood functions are calculated globally for the cross section and on an event-by-event basis for the energy and angular distributions. All the terms in the likelihood function contribute substantially in the case of $\Delta\kappa_\gamma$ whereas the result for λ_γ is dominated by the sensitivity to the shape in Region 2. The $(-\Delta\log\mathcal{L})$ functions obtained for $\Delta\kappa_\gamma$ fitted at $\lambda_\gamma = 0$, and for λ_γ fitted at $\Delta\kappa_\gamma = 0$, are shown in Figure 6.

At present energies, the contributions of the cross section and of the shape variation terms are equally important for the fit of $\Delta\kappa_\gamma$. The results are:

$$\begin{aligned} \Delta\kappa_\gamma &= 0.4 \pm 0.7(\mathrm{stat}) \pm 0.2(\mathrm{syst}) \quad \text{assuming} \quad \lambda_\gamma = 0 \\ \lambda_\gamma &= 0.3 \pm 0.9(\mathrm{stat}) \pm 0.2(\mathrm{syst}) \quad \text{assuming} \quad \Delta\kappa_\gamma = 0 \end{aligned}$$

where the errors correspond to an increase of $-\log\mathcal{L}$ by 0.5. The lower precision for λ_γ is expected since the exchanged W's are at a rather low momentum scale and the λ_γ term in the Lagrangian contains high powers of the W momentum. The 68% and 95% confidence level contours in the $(\Delta\kappa_\gamma, \lambda_\gamma)$ plane from a two-parameter fit, are shown in Figure 7 The two parameters are not independent, however the confidence level contours are only slightly tilted due to the fact that the results are not far from the SM values. The correlation factor found in the 2D fit is 0.2 .

The estimation of the systematic uncertainties follows the procedure described in [16]. It leads to a systematic error of ± 0.2 on both parameters.

The 95% C.L. limits derived for the one parameter fits, including systematic errors, are :

$$-1.0 < \Delta\kappa_\gamma < 1.7 \quad \text{assuming} \quad \lambda_\gamma = 0$$
$$-1.5 < \lambda_\gamma < 2.0 \quad \text{assuming} \quad \Delta\kappa_\gamma = 0.$$

The validity of these 95% C.L. limits and the error from the likelihood fit have been checked using the procedure described in [16].

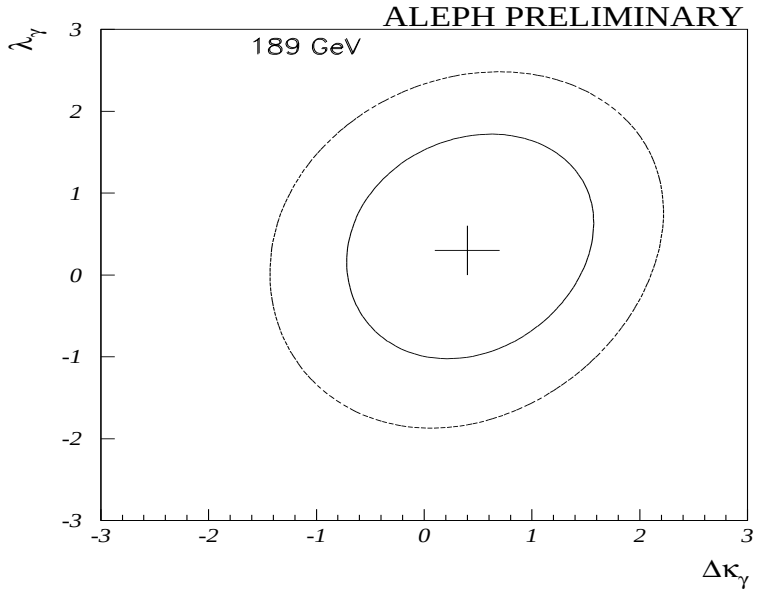

Figure 7: The 68% (full line) and 95% (dashed line) confidence level contours in the $\Delta\kappa_\gamma, \lambda_\gamma$ plane.

7 Hard collinear photons

7.1 Event selection and the process $e^+e^- \to \gamma\gamma(\gamma)$

An acceptance for events from the process $e^+e^- \to \gamma\gamma(\gamma)$ is defined to include events with at least two photons with polar angles such that $|\cos\theta| < 0.95$ and energies above $0.25\sqrt{s}$ where the angle between the two most energetic photons is at least 160°. The background from Bhabha scattering is greatly reduced by allowing at most one converted photon per event and requiring that there be no tracks in the event, besides those associated with that photon. Cosmic ray events which traverse the detector are eliminated if they leave hits in the outer part of the HCAL or if their measured interaction time is inconsistent with a beam crossing. fThe efficiency of this selection for events within the acceptance is 84%.

When the above selection is applied to the 188.6 GeV data sample 1309 events are selected consistent with the Monte Carlo prediction of 1388 events.

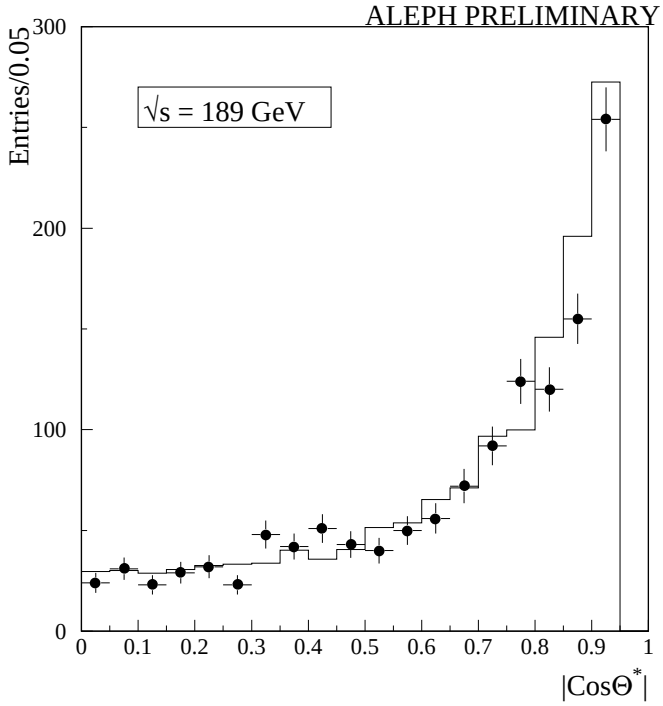

Figure 8: *Predicted and observed lowest-order differential cross section as a function of* $\cos\theta^*$ *for the reaction* $e^+e^- \to \gamma\gamma$*. The predicted distribution includes a small contribution from the Bhabha background. The errors shown here are purely statistical.*

In this sample 65 events have one or more additional photons with energy above 1 GeV inside the angular range $|\cos\theta| < 0.95$, compared with an expectation of 74 events. Two events are observed in the data with four photons in agreement with a Monte Carlo expectation of 4 events. No events are observed with more than four photons.

The lowest order differential cross section for electron-positron annihilation into two photons is given by

$$\left(\frac{\mathrm{d}\sigma}{\mathrm{d}\Omega}\right)_{\mathrm{Born}} = \frac{\alpha^2}{s}\left(\frac{1+\cos^2\theta}{1-\cos^2\theta}\right).$$

The observed cross section is modified by two effects: higher order processes, in particular initial state radiation, and detector effects. Due to initial state radiation, the centre-of-mass frame of the two detected photons is not necessarily at rest in the laboratory. The events are therefore transformed into the two-photon rest frame to define the production angle θ^*. The distribution of this production angle is shown for both data and Monte Carlo expectations in Figure 8. The measured cross section for events inside the acceptance is

$$\sigma(e^+e^- \to \gamma\gamma(\gamma)) = 9.13 \pm 0.25 \pm 0.18\,\mathrm{pb}.$$

.

The systematic uncertainty in the above cross section estimates includes contributions from the various sources listed in Table 2. The uncertainties coming from the photon selection efficiency are measured as in the single photon analysis. The uncertainty in the level of the Bhabha background

Table 2: *Systematic uncertainties in the* $e^+e^- \to \gamma\gamma$ *analysis.*

Source	Uncertainty (%)
Photon selection	1.2
Converted photon selection	0.6
Background	0.8
Integrated luminosity	0.5
Monte Carlo statistical	1.1
Monte Carlo theoretical	< 1.0
Total (in quadrature)	2.2

is estimated to be 0.8%. The effect of missing higher orders in the Monte Carlo is estimated to be less than 1.0%. This estimate is obtained by comparing the number of observed and selected events in a high statistics data sample recorded at the Z peak. Added in quadrature, the total systematic uncertainty is 2.2%.

7.2 QED cutoff parameters

Possible deviations from QED are usually characterised by cutoff parameters Λ_+ and Λ_- corresponding to a modified differential cross section

$$\frac{\mathrm{d}\sigma}{\mathrm{d}\Omega} = \left(\frac{\mathrm{d}\sigma}{\mathrm{d}\Omega}\right)_{\mathrm{QED}} \left[1 \pm \frac{s^2}{2\Lambda_\pm^4}(1-\cos^2\theta^*)\right].$$

In order to extract limits on the parameters Λ_+ and Λ_- a binned maximum likelihood fit is performed on the background-subtracted $\cos\theta^*$ distribution under the assumption that it contains contributions from both QED and the cutoff interaction. A bin-by-bin correction is made to take into account the detector efficiency. Since the $\cos\theta^*$ distribution of the cutoff interaction is only known to lowest order, a further bin-by-bin correction is made by comparing the third order QED distribution to the corresponding lowest order distribution. This assumes that the effect of higher order corrections is the same for the basic QED process and for possible new physics processes. The systematic uncertainty of 2.2% on the level of Standard Model background is taken into account in the fit. The limit on Λ_+ (Λ_-) is obtained by integrating the likelihood distribution over the physically allowed region $\Lambda_+ > 0$ ($\Lambda_- > 0$). The 95% C.L. lower limits obtained for Λ_+ and Λ_- are 309 GeV and 269 GeV, respectively. Figure 9 shows the ratio of the observed cross section to that predicted by QED, as a function of $\cos\theta^*$. Also indicated, as dotted lines, are the modified cross sections corresponding to the 95% C.L. lower limits on Λ_+ and Λ_-.

7.3 Contact interactions

An alternative description of extensions to QED is provided by effective Lagrangians, which contain non-standard couplings of the form γe^+e^- and $\gamma\gamma e^+e^-$. The lowest order effective Lagrangians, describing these interactions, contain operators of order 6, 7 and 8. These lead to modified differential cross sections of the form [28]

$$\left(\frac{\mathrm{d}\sigma}{\mathrm{d}\Omega}\right)_{\mathrm{QED+6}} = \left(\frac{\mathrm{d}\sigma}{\mathrm{d}\Omega}\right)_{\mathrm{QED}} \left[1 + \frac{s^2}{\alpha\Lambda_6^4}(1-\cos^2\theta^*)\right],$$

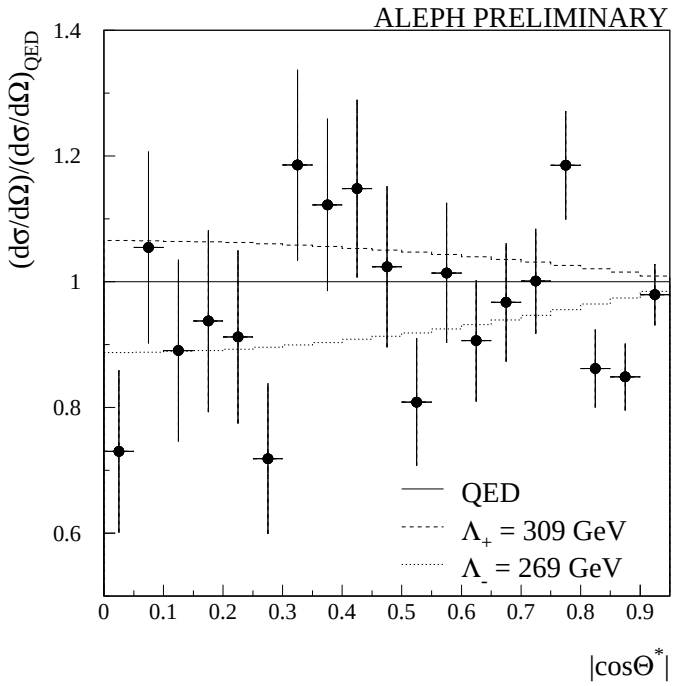

Figure 9: *The ratio of the observed to predicted cross sections, for the process* $e^+e^- \to \gamma\gamma(\gamma)$*, as a function of* $\cos\theta^*$*. Also shown are the 95% C.L. level limits on the QED cutoff model.*

$$\left(\frac{d\sigma}{d\Omega}\right)_{\mathrm{QED+7}} = \left(\frac{d\sigma}{d\Omega}\right)_{\mathrm{QED}} + \frac{s^2}{32\pi\Lambda_7^6},$$
$$\left(\frac{d\sigma}{d\Omega}\right)_{\mathrm{QED+8}} = \left(\frac{d\sigma}{d\Omega}\right)_{\mathrm{QED}} + \frac{s^2 m_e^2}{32\pi\Lambda_8^8}.$$

Fits are performed to extract limits on these parameters using the procedure outlined above. The 95% C.L. lower limits obtained for Λ_6, Λ_7 and Λ_8 are 1259 GeV, 686 GeV and 20.1 GeV, respectively.

7.4 Limits on M_{e^*}

The reaction $e^+e^- \to \gamma\gamma$ can also proceed via the t-channel exchange of an excited electron. In this case the cross section depends on two parameters: the mass M_{e^*} of the excited electron and the $ee^*\gamma$ coupling. The simplest gauge-invariant form [29] of the interaction (the Low Lagrangian) leads to the differential cross section given in [30]. A fit is performed as above and a 95% C.L. lower limit on M_{e^*} of 335 GeV/c^2 is obtained in the case of equal $ee^*\gamma$ and $ee\gamma$ couplings.

8 Conclusions

Single- and multi-photon production is studied in the ALEPH data collected at centre-of-mass energies up to 188.6 GeV. The cross sections for the processes $e^+e^- \to \nu\bar{\nu}\gamma(\gamma)$ and $e^+e^- \to \gamma\gamma(\gamma)$ are measured and are found to be compatible with the expectations for the Standard Model.

The data from the photon(s) and missing energy analyses are used to derive cross section upper limits for the processes $e^+e^- \to XY \to YY\gamma$, $e^+e^- \to \tilde{G}\tilde{G}\gamma$ and $e^+e^- \to XX \to YY\gamma\gamma$. A cross section upper limit of 0.27 pb is obtained of the $e^+e^- \to \tilde{G}\tilde{G}\gamma$ process. From this cross section upper limits a 95% C.L. lower limit of $1.0 \times 10^{-5}\,\mathrm{eV}/c^2$ at 95% C.L. is set on the mass of the gravitino. The lower limit on the χ_2^0 mass as a function of selectron mass is determined and compared to the region compatible with the CDF event for the neutralino LSP scenario. In the gravitino LSP scenario, studied in [9], the χ_1^0 mass is found to be greater that $91\,\mathrm{GeV}/c^2$.

Events with one or more photons and missing energy are also used to measure the anomalous WWγ couplings parameters $\Delta\kappa_\gamma$ and λ_γ. These are $0.4 \pm 0.7(\mathrm{stat}) \pm 0.2(\mathrm{syst})$ and $0.3 \pm 0.9(\mathrm{stat}) \pm 0.2(\mathrm{syst})$, in the case of a one parameter fit, respectively.

The data from the hard collinear photon analysis are used to place limits on the parameters of a number of extensions to the Standard model, notably the presence of $e^+e^-\gamma\gamma$ contact interactions and the exchange of a massive excited electron in the t-channel. The 95% C.L. lower limits on the QED cutoff parameters Λ_+ and Λ_- are 309 GeV and 269 GeV, respectively. The effect of excited electron exchange depends on both the mass and coupling constant. In the simplest case, an assumption that the $ee^*\gamma$ coupling is equal to the $ee\gamma$ coupling yields a 95% C.L. lower limit on M_{e^*} of $335\,\mathrm{GeV}/c^2$.

References

[1] ALEPH Collaboration, Phys. Lett. **B420** (1998) 127;
ALEPH Collaboration, Phys. Lett. **B427** (1998) 201.

[2] JADE Collaboration, Phys. Lett. **B139** (1984) 327;
MAC Collaboration, Phys. Rev. **D33** (1986) 3472;
CELLO Collaboration, Phys. Lett **B215** (1988) 186;
VENUS Collaboration, Z. Phys **C45** (1989) 175;
ASP Collaboration, Phys. Rev. **D39** (1989) 3207;
TOPAZ Collaboration, Phys. Lett. **B361** (1995) 199;
DELPHI Collaboration, Eur. Phys. J. **C1** (1998) 1;
DELPHI Collaboration, Eur. Phys. J. **C6** (1999) 371;
L3 Collaboration, Phys. Lett. **B444** (1998) 503;
OPAL Collaboration, Eur. Phys. J. **C2** (1998) 597;
OPAL Collaboration, CERN-PPE/98-143, submitted to Phys. Lett. **B**.

[3] H. Komatsu and J. Kumo, Phys. Lett. **B157** (1985) 90.

[4] H. Haber and D. Wyler, Nucl. Phys. **B323** (1989) 267.

[5] S. Ambrosanio et al., Phys. Rev. **D55** (1997) 1372.

[6] P. Fayet, Phys. Lett. **B69** (1977) 489, **B70** (1977) 461;
M. Dine, W. Fischler and M. Srednichi, Nucl. Phys. **B189** (1981) 575;
M. Dine, A. Nelson and Y. Shirman, Phys. Rev. **D51** (1995) 1362;
S. Dimopoulos, S. Thomas and J. D. Wells, Nucl. Phys. **B488** (1997) 39.

[7] S. Dimopoulos et al., Phys. Rev. Lett. **76** (1996) 3494.

[8] S. Dimopoulos, S. Thomas and J. D. Wells, Phys. Rev. **D54** (1996) 3283.

[9] ALEPH Collaboration, "Search for Gauge Mediated SUSY Breaking topologies at $\sqrt{s} = 189\,\mathrm{GeV}$",ALEPH CONF 99-002 (`http://alephwww.cern.ch`).

[10] A. Brignole, F. Feruglio and F. Zwirner, Nucl. Phys. **B516** (1998) 13.

[11] CDF Collaboration, Phys. Rev. Lett. **81** (1998) 1791.

[12] D0 Collaboration, Phys. Rev. Lett. **80** (1998) 442.

[13] *Triple Gauge Couplings*, G. Gounaris *et al*, in *Physics at LEP2*, G. Altarelli, T. Sjöstrand and F. Zwirner, editors, CERN 96-01 (1996) 525.

[14] ALEPH Collaboration, *Measurement of Triple Gauge-Boson Couplings at 172 GeV*, *Phys. Lett.* **B422** (1998) 369.

DELPHI Collaboration, *Measurement of Trilinear Gauge Couplings in* $\mathrm{e^+e^-}$ *collisions at 161 GeV and 172 GeV*, *Phys. Lett.* **B423** (1998) 194.

L3 Collaboration, *Production of single W bosons in* e^+e^- *interactions at* $130 < \sqrt{s} < 183$ *GeV and limits on anomalous* $WW\gamma$ *couplings*, *Phys. Lett.* **B436** (1998) 417.

OPAL Collaboration, W^+W^- *production and triple gauge boson couplings at LEP energies up to 183 GeV*, CERN EP/98-167, to be published in Eur. Phys. Journal C.

[15] The D0 Collaboration, S. Abachi *et al*, *Phys. Rev.* **D58** (1998) 3102.

[16] ALEPH Collaboration, *Measurement of triple gauge $WW\gamma$ couplings at LEP2 using photonic events*, *Phys. Lett.* **B445** (1998) 239.

[17] PLUTO Collaboration, Phys. Lett. **B59** (1980) 87;
JADE Collaboration, Z. Phys. **C19** (1983) 197;
MARKJ Collaboration, Phys. Rev. Lett. **53** (1984) 134;
TASSO Collaboration, Z. Phys. **C26** (1984) 337;
CELLO Collaboration, Phys. Lett. **B168** (1986) 420;
HRS Collaboration, Phys. Rev. **D34** (1986) 3286;
MAC Collaboration, Phys. Rev. **D35** (1987) 1;
VENUS Collaboration, Z. Phys. **C45** (1989) 175;
TOPAZ Collaboration, Phys. Lett. **B284** (1992) 144;
AMY Collaboration, Phys. Lett. **B303** (1993) 385;
DELPHI Collaboration, Phys. Lett. **B433** (1998) 429;
L3 Collaboration, Phys. Lett. **B413** (1997) 159;
OPAL Collaboration, Phys. Lett. **B438** (1998) 379.

[18] ALEPH Collaboration, Nucl. Instrum. Methods **A294** (1990) 121.

[19] ALEPH Collaboration, Nucl. Instrum. Methods **A360** (1995) 481.

[20] S. Jadach, B. F. L. Ward and Z. Was, Comp. Phys. Commun. **79** (1994) 503,
A. Jacholkowska, J. Kalinowski, and Z. Was, "Higher-order QED corrections to $e^+e^- \to \nu\bar{\nu}\gamma$ at LEP2", HEP-PH/9803375, submitted to Eur. Phys. Journal. C.

[21] D. R. Yennie, S. C. Frautschi and H. Suura, Annals of Phys. **13** (1961) 379.

[22] G. Montagna et al., "Single- and multi-photon final states with missing energy at e^+e^- colliders", hep-ph/9807465.

[23] F. A. Berends and R. Kleiss, Nucl. Phys. **B186** (1981) 22.

[24] P. Janot, Tests of QED to $O(\alpha^3)$ and $O(\alpha^4)$ and a search for excited leptons, using the CELLO detector at PETRA, Ph.D. Thesis, LAL 87-31 (1987).

[25] S. Katsanevas and S. Melachroinos, in *Physics at LEP2*, Eds. G. Altarelli, T. Sjöstrand, F. Zwirner, CERN Report 96-01, Volume 2 (1996) 328.

[26] S. Jadach, W. Placzek and B. F. L. Ward, Phys. Lett. **B390** (1997) 298.

[27] J. F. Grivaz and F. Le Diberder, LAL 92-37 (1992).

[28] O. J. P. Eboli et al., Phys. Lett. **B271** (1991) 274.

[29] F. E. Low, Phys. Rev. Lett. **14** (1965) 238.

[30] A. Litke, Experiments with electron-positron colliding beams, Ph.D. Thesis, Harvard Univ (1970).